PHYSICAL REVIEW E VOLUME 58, NUMBER 2 AUGUST 1998

Nonlocal pseudopotential calculation for the electron-ion correlation in liquid metals

S. K. Lai,[1,2] K. Horii,[1] and M. Iwamatsu[1]
[1]Department of Computer Engineering, Faculty of Information Sciences, Hiroshima City University, 3-4-1 Ozuka-higashi, Asaminami-ku, Hiroshima 731-31, Japan
[2]Department of Physics, National Central University, Chung-li 320, Taiwan, Republic of China

(Received 2 March 1998)

A full nonlocal model potential is employed to calculate the screened electron charge density $n^{\mathrm{EC}}(q)$ and to construct the interatomic pair potential, which is then used in the modified hypernetted-chain integral equation to determine the ion-ion static structure factor $S_{ii}(q)$. These two basic quantities are subsequently used as input data for the calculation of the electron-ion correlation. For the simple liquid metals Na, Mg, and Al, our calculated electron-ion structure factors $S_{ei}(q)$ agree very well with the positions of extrema of the experimental or computer-simulated $S_{ei}(q)$. Quantitative analysis of the two main contributions, $n^{\mathrm{EC}}(q)$ and $S_{ii}(q)$, shows that $S_{ei}(q)$ obtained in a full nonlocal pseudopotential theory is in general different from that in the local pseudopotential theory. Such disparities in the two theoretical frameworks arise from the nonlocality of electron-ion pseudopotential, which, for a quantitative study, should be incorporated in the theory especially when one is treating the correlations of electrons and ions on an equal footing. At the level of achievement attained in this work, there is now a greater hope of understanding the electron-ion correlations if experimental errors for $S_{ei}(q)$ are considerably reduced. [S1063-651X(98)09208-3]

PACS number(s): 61.25.Mv, 61.20.Gy

I. INTRODUCTION

Coulomb interaction between charged bodies is one of the basic forces in nature. Liquid metal represents one simple example whose constituents, ions and electrons, display classical as well as quantum mechanical behaviors. Over the last twenty years tremendous efforts have been devoted to studying various physical properties of this system. In many of these applications one notices a common practice in that the role of valence electrons, which is one of the two components in a liquid metal, has not been put on an equal footing as ions. Instead one takes advantage of the electronic mass and its degenerate physical property to eliminate this degree of freedom in mathematical formulation. Thus the two-component nature of a liquid metal is commonly seen to be reduced to an effectively one-component system. Such a picture for the liquid metal as a collection of weakly interacting pseudoatoms has been widely accepted by the liquid-state community and was applied in a different context over the last two decades. Recently there has been a revived interest both theoretically and experimentally in understanding the inherent two-component nature of a liquid metal. Experimentally there are now high resolution liquid structure data for liquid metals by neutron scattering [1] and these data when combined with those of x rays and with theoretical results for the electron-electron correlations allow an extraction of the electron-ion structure factor $S_{ei}(q)$ to a reasonable precision. In this connection one should draw attention to some recent developments in the homogeneous electron gas theories. These more refined theories [2–4], which generally recourse to the tool of quantal simulation, handle more accurately the classic problem of the electron-electron exchange-correlation (EC) effects. Progressing almost in parallel is the extensive use of computer simulations such as the Car-Parrinello molecular dynamics technique [5,6], which was applied quite successfully to study the correlations between valence electrons and ions in the liquid metal. These computer-simulated experiments supplement the existing laboratory experiments and have elucidated many structural features pertinent to electrons and ions. It is therefore appropriate and of great theoretical interest at this time to revisit this interesting problem of the partial liquid structure factors of liquid metals that consist of electron-electron, electron-ion, and ion-ion correlations.

The interest in the two-component nature of liquid metals originates from the pioneering work of Cowan and Kirkwood [7]. These authors described the liquid metal as being composed of two types of charged interacting particles and they presented results for the partial structure factors of the electrons and ions that are valid in a somewhat restrictive regime. Their work has subsequently been further elaborated by Tosi and March [8] who discussed the issue from a many-body point of view focusing more on electrons. In fact explicit expressions for the partial structure factors and their inter-relations in some limiting cases were derived concurrently by Watabe and Hasegawa [9] using the Green function method and by Chihara [10] employing the integral equation approach. A similar effort has been reported by Trigger [11] using an approach in close analogy with that of Watabe and Hasegawa [9]. Despite these fundamental studies progress in understanding the intrinsic two-component nature of the liquid metal seems to be slow. Beginning in the early 1990s systematic neutron scattering experiments have been carried out by Takeda *et al.* [1] who combined their neutron data with those of x rays and of theoretical many-body results of the interacting electron gas to deduce specifically the electron-ion partial structure factors and the valence electron charge distribution for a number of *sp*-type liquid metals. Such experimental endeavors are extremely difficult and delicate since both x-ray and neutron scattering data *a priori* have to be taken with high accuracy for the extracted electron-ion structure factor $S_{ei}(q)$ to be reliable. In connection with the assessment of the experimental $S_{ei}(q)$, it may be worthwhile to remark that there already appear in the literature critical comments on getting high quality results [12]. Concurrently, there are extensive works on computer simulations whose studies provide direct information on the electron-ion correlations in liquid metals. The comparison of the latter with laboratory data have given us a much better picture on the electron-ion interactions. It is the purpose of this paper to attempt to interpret some of these measured data theoretically.

In this work the electron-ion structure factor is calculated following the same means as used by Tosi and March [8], Trigger [11], and others [13,14]. The method is essentially a perturbative approach assuming a weak interaction between electrons and ions. Since the electron-ion pseudopotential for the *sp*-type liquid metals considered here can be considered to be weak, the use of the linear response approximation for studying $S_{ei}(q)$ should be reasonably justified [15] provided quantities involved can be accurately and reliably obtained. We show in this work that our nonlocal model pseudopotential [16,17], combined with recent theoretical results in the homogeneous interacting electron gas, describes quite well the microscopic correlations between conduction electrons and ions. Differing from previous works [8,13,14], we shall discuss in some detail the screened valence electron charge density within the nonlocal pseudopotential. We reexamine the approximations applied to the electron charge density that have not been discussed much in the literature for lack of a detailed knowledge of the electron distribution in the ion cores. The paper is organized as follows. In Sec. II we give a brief documentation of the expressions for $S_{ei}(q)$ derived within the functional derivative method. Next, we describe with a fair amount of detail the generalized energy independent nonlocal model pseudopotential (EINMP) theory for the calculation of the screened electron charge density. Here, we draw attention to some approximations in the nonlocal pseudopotential that we have made and applied successfully in previous applications [18]. Then, we introduce the modified hypernetted-chain theory to the study of the ion-ion static structure factor. Numerical results for the screened charge density, $S_{ii}(q)$ and $S_{ei}(q)$ are the content of Sec. III. Here discussion of their characteristic features will be given. Finally in Sec. IV we summarize our main results.

II. THEORY

In this section we first present the equation for $S_{ei}(q)$ within the functional derivative method. Then we review the generalized EINMP theory [16] deriving an expression for the screened electron charge density that is needed in the calculation of $S_{ei}(q)$. Finally we summarize the essential equations appearing in the integral equation approach to the ion-ion static structure factor.

A. Electron-ion structure factor

Following the work of Cusack *et al.* [19], let us begin with the density-density time correlation function for the electron $n(\mathbf{r}t)$ and ion $\rho_i(\mathbf{r}t)$, which is defined as

$$\langle n(\mathbf{r}_1 t_1)\rho_i(\mathbf{r}_2 t_2)\rangle_c = \langle n(\mathbf{r}_1 t_1)\rho_i(\mathbf{r}_2 t_2)\rangle - \langle n(\mathbf{r}_1 t_1)\rangle\langle \rho_i(\mathbf{r}_2 t_2)\rangle, \quad (1)$$

where the subscript *c* means the cumulant average. The functional derivative method is essentially a perturbative approach aimed at generating a series of perturbation expansion for $\langle \mathcal{T}[n(\mathbf{r}_1 t_1)\rho_i(\mathbf{r}_2 t_2)]\rangle_c$, $\mathcal{T}$ being the time-ordered operator. If one assumes the electron-ion interaction $W_{ei}(\mathbf{x}-\mathbf{y})$ as an external potential, the functional derivative method gives for the first and second order terms

$$\begin{aligned}\delta^{(1)}\langle \mathcal{T}[n(\mathbf{r}_1 t_1)\rho_i(\mathbf{r}_2 t_2)]\rangle_c &= -(i/\hbar)\int \langle \mathcal{T}[n(\mathbf{r}_1 0)n(\mathbf{x}t)]\rangle_c \langle \mathcal{T}[\rho_i(\mathbf{r}_2 0)\rho_i(\mathbf{y}t)]\rangle_c W_{ei}(\mathbf{x}-\mathbf{y})d\mathbf{x}\, d\mathbf{y}\, dt \\ &= \varrho_i^2 \int \chi_{ee}^{(1)}(\mathbf{r}_1,\mathbf{x}) S_{ii}(\mathbf{y}-\mathbf{r}_2) W_{ei}(\mathbf{x}-\mathbf{y}) d\mathbf{x}\, d\mathbf{y} \end{aligned} \quad (2)$$

and

$$\begin{aligned}\delta^{(2)}\langle \mathcal{T}[n(\mathbf{r}_1 t_1)\rho_i(\mathbf{r}_2 t_2)]\rangle_c &= \frac{1}{2}\left(-\frac{i}{\hbar}\right)^2 \int \langle \mathcal{T}[n(\mathbf{r}_1 0)n(\mathbf{x}t)n(\mathbf{x}'t')]\rangle_c \langle \mathcal{T}[\rho_i(\mathbf{r}_2 0)\rho_i(\mathbf{y}t)\rho_i(\mathbf{y}'t')]\rangle_c \\ &\quad \times W_{ei}(\mathbf{x}-\mathbf{y})d\mathbf{x}\, d\mathbf{y} W_{ei}(\mathbf{x}'-\mathbf{y}')d\mathbf{x}'\, d\mathbf{y}' \\ &= \frac{\varrho_i^3}{2}\int \chi_{ee}^{(2)}(\mathbf{r}_1,\mathbf{x},\mathbf{x}') S_{iii}(\mathbf{r}_2,\mathbf{y},\mathbf{y}') W_{ei}(\mathbf{x}-\mathbf{y}) W_{ei}(\mathbf{x}'-\mathbf{y}') d\mathbf{x}\, d\mathbf{y}\, d\mathbf{x}'\, d\mathbf{y}', \end{aligned} \quad (3)$$

where ϱ_i is the mean ionic number density, $\chi_{ee}^{(1)}$ and $\chi_{ee}^{(2)}$ are the linear and quadratic density response functions for jellium, and S_{ii} and S_{iii} are the two and three particle correlation functions, respectively. For numerical computation it is more convenient to Fourier transform Eqs. (2) and (3). Doing this we obtain

$$\begin{aligned} S_{ei}(q) = {} & W_{ei}(q)\chi_{ee}^{(1)}(q)S_{ii}(q)/\sqrt{Z} \\ & + \frac{1}{2}\int \chi_{ee}^{(2)}(q)S_{iii}(q,q'-q,-q')W_{ei}(q') \\ & \times W_{ei}(q-q')dq'/(2\pi)^3. \end{aligned} \tag{4}$$

Since S_{iii} is generally less understood and its numerical accuracy is more uncertain theoretically, we shall thus confine our discussion to the first order term assuming therefore a weak W_{ei} [15]. It is interesting to note that the factor multiplying $S_{ii}(q)/\sqrt{Z}$ is essentially the screened electron charge density $n^{\mathrm{EC}}(q)$ [8], which will be derived below. Thus, to first order in the electron-ion pseudopotential, we obtain

$$S_{ei}(q) = \frac{n^{\mathrm{EC}}(q)S_{ii}(q)}{\sqrt{Z}}, \tag{5}$$

which is the expression to be used in the following calculation.

B. Model pseudopotential: Screened electron charge density

1. Nonlocal model pseudopotential

We begin with the Poisson's equation for the total valence electron density $n(\mathbf{r}) = n_0 + \delta n(\mathbf{r})$ where $\delta n(\mathbf{r})$ is the change in electron density from the mean value n_0 due to the perturbation of ions. The corresponding total electronic potential $V_e(\mathbf{r})$ will accordingly be written as $V_e(\mathbf{r}) = V_{e,0} + \delta V_e(\mathbf{r})$ where $V_{e,0}$ is an average potential for all of the valence electrons. Substituting $\delta n(\mathbf{r})$ and $\delta V_e(\mathbf{r})$ into the Poisson's equation

$$\nabla^2 \delta V_e(\mathbf{r}) = -4\pi\delta n(\mathbf{r}) \tag{6}$$

and applying the Fourier transformation to $\delta V_e(\mathbf{r})$ and $\delta n(\mathbf{r})$, it can be shown in the nonlocal pseudopotential theory

$$\langle \mathbf{k}+\mathbf{q}|V_e(\mathbf{r})|\mathbf{k}\rangle \equiv \wp(q)v_e(q) = \frac{4\pi}{q^2}\langle \mathbf{k}+\mathbf{q}|n(\mathbf{r})|\mathbf{k}\rangle, \quad q \neq 0, \tag{7}$$

where $\wp(q) = N^{-1}\Sigma_\lambda e^{-i\mathbf{q}\cdot\mathbf{R}_\lambda}$, N being the total number of ions in the system. To proceed, we write the total valence electron density $n(\mathbf{r})$ as [17]

$$n(\mathbf{r}) = \sum_{\mathbf{k}} \chi_{\mathbf{k}}^*(\mathbf{r})\chi_{\mathbf{k}}(\mathbf{r}) + \sum_{\mathbf{k}} [\psi_{\mathbf{k}}^*(\mathbf{r})\psi_{\mathbf{k}}(\mathbf{r}) - \chi_{\mathbf{k}}^*(\mathbf{r})\chi_{\mathbf{k}}(\mathbf{r})], \tag{8}$$

where $\chi_{\mathbf{k}}(\mathbf{r})$ and $\psi_{\mathbf{k}}(\mathbf{r})$ are respectively the pseudo and true wave functions. In Eq. (8) the second term accounts for the difference between the true and pseudo charge densities and is more conveniently expressed as

$$\begin{aligned} \sum_\lambda \rho(\mathbf{r}-\mathbf{R}_\lambda) = \sum_\lambda \sum_{\mathbf{k}} \{ & \psi_{\mathbf{k}}^*(\mathbf{r}-\mathbf{R}_\lambda)\psi_{\mathbf{k}}(\mathbf{r}-\mathbf{R}_\lambda) \\ & - \chi_{\mathbf{k}}^*(\mathbf{r}-\mathbf{R}_\lambda)\chi_{\mathbf{k}}(\mathbf{r}-\mathbf{R}_\lambda)\}, \end{aligned} \tag{9}$$

where $\rho(\mathbf{r}-\mathbf{R}_\lambda)$ vanishes for $|\mathbf{r}-\mathbf{R}_\lambda| > \mathcal{R}_c$, where $\mathcal{R}_c$ is the ion core radius. We should emphasize that there is an arbitrariness in the choice of $\mathcal{R}_c$ within which the depletion charge density distributes. We shall return to this parameter in the following discussion. To continue our calculation of $n(\mathbf{r})$, we can either expand $\chi_{\mathbf{k}}(\mathbf{r})$ as many others (for instance, by Wax *et al.* [14]) by a low order perturbation, or as Li, Li, and Wang [16] by a formal treatment of the choice of the perturbation potential (see [16] and also [15] for further quantitative details) by a higher order perturbation. Normalizing the true charge density $\langle\psi|\psi\rangle = 1$ as usual [17], $\langle \mathbf{k}+\mathbf{q}|n(\mathbf{r})|\mathbf{k}\rangle$ can be shown to read

$$\begin{aligned} \langle \mathbf{k}+\mathbf{q}|n(\mathbf{r})|\mathbf{k}\rangle = {} & \wp(q)\left[\frac{1}{2\pi^3}\int_{k\leqslant k_F} d^3k\, \frac{|N_{\mathbf{k}}|^2 w_q(\mathbf{k})}{E_{\mathbf{k}}^{(0)} - E_{\mathbf{k}+\mathbf{q}}^{(0)}}\right] \\ & + \wp(q)\rho_q, \end{aligned} \tag{10}$$

where $E_{\mathbf{k}}^{(0)}$ is the unperturbed energy and $|N_{\mathbf{k}}|^2$ is a renormalization constant such that $\langle\psi|\psi\rangle = 1$. Here $w_{\mathbf{q}}(\mathbf{k}) = \langle \mathbf{k}+\mathbf{q}|w(\mathbf{r})|\mathbf{k}\rangle$ is the screened electron-ion nonlocal pseudopotential and

$$\rho_q = \Omega_0^{-1}\int_{\Omega_c} e^{-i\mathbf{q}\cdot\mathbf{r}}\rho(\mathbf{r})d^3r \tag{11}$$

in which Ω_0 is the atomic volume and $\Omega_c = 4\pi\mathcal{R}_c^3/3$ is the ion-core volume over which the depletion charge density is to be integrated. At this point it is appropriate to remark that, although the calculation of ρ_q, in principle, can be effected by analytical continuation of the wave functions into Ω_c using the known magnitude and derivatives of these functions on the Ω_c surface, it is, however, practically intractable by the presence of the exponential term. In view of this, we have followed Shaw and Harrison [20] by making two successive approximations. The first approximation is to ignore the q dependence of the integral of Eq. (11) leading to

$$\rho_d = (\Omega_0/\pi^2)\int_0^{k_F} dk\, k^2|N_{\mathbf{k}}|^2(|N_{\mathbf{k}}|^{-2} - 1). \tag{12}$$

The associate potential is thus $4\pi\rho_d/(\Omega_0 q^2)$. This approximation is equivalent to assuming that the depletion charge density is a point charge at the ion position. Once ρ_d is evaluated numerically the second approximation is to regard the depletion hole charge to have some form of distribution within Ω_c stressing its deviation from pointlike. Now, according to Shaw and Harrison [20], one accounts for such deviation by introducing a modulation function *M(q)*. In this way, we write the depletion hole potential as $v_{dq} = 4\pi\rho_d M(q)/(\Omega_0 q^2)$, although the exact form of $M(q)$ is in principle not known. Since in the present work our interest is on the correlations between valence electrons and ions, an appropriate study of the choice of $M(q)$ is certainly crucial and important for understanding the electronic charge density around ions. It should be noted here that the significance of $M(q)$ in accounting for the metallic properties has been previously discussed by several authors [21–23]. Given Eq. (10) for $\langle \mathbf{k}+\mathbf{q}|n(\mathbf{r})|\mathbf{k}\rangle$, the corresponding $v_e(q)$ in Eq. (7) can be written as

$$\begin{aligned} v_e(q) &= \frac{2}{\pi^2 q^2} \int_{k\leqslant k_F} d^3k \, \frac{|N_\mathbf{k}|^2 w_q(\mathbf{k})}{E_\mathbf{k}^{(0)} - E_{\mathbf{k}+\mathbf{q}}^{(0)}} + v_{dq} \\ &= v_s(q) + v_{dq}, \end{aligned} \tag{13}$$

where we have denoted the screened potential per ion by $v_s(q)$. Our next task is to find $w_\mathbf{q}(\mathbf{k})$. This can be done by noting that the total screened electron-ion form factor $W(\mathbf{r}) = \Sigma_\lambda w(\mathbf{r}-\mathbf{R}_\lambda)$ and the total bare electron-ion form factor $W^b(\mathbf{r}) = \Sigma_\lambda w^b(\mathbf{r}-\mathbf{R}_\lambda)$ are related by $\langle \mathbf{k}+\mathbf{q}|W(\mathbf{r})|\mathbf{k}\rangle = \langle \mathbf{k}+\mathbf{q}|W^b(\mathbf{r})|\mathbf{k}\rangle + \langle \mathbf{k}+\mathbf{q}|V_e(\mathbf{r})|\mathbf{k}\rangle$ and, in consultation of Eqs. (7) and (13), can be written as [17]

$$\langle \mathbf{k}+\mathbf{q}|W(\mathbf{r})|\mathbf{k}\rangle \equiv \wp(q) w_\mathbf{q}(\mathbf{k}) = \wp(q)[w_\mathbf{q}^b(\mathbf{k}) + v_s(q) + v_{dq}]. \tag{14}$$

For our generalized EINMP, $w_\mathbf{q}^b(\mathbf{k}) = v_q + f(\mathbf{k}+\mathbf{q},\mathbf{k})$ where $v_q = -4\pi Z/(\Omega_0 q^2)$, Z being the nominal valence, is the state-independent part of the ionic model pseudopotential and $f(\mathbf{k}+\mathbf{q},\mathbf{k})$ is the state-dependent part. Notice that $w_\mathbf{q}(\mathbf{k})$ appears also in $v_s(q)$ [see Eq. (13)] and hence has to be solved self-consistently with Eq. (14). The result is

$$\begin{aligned} w_\mathbf{q}(\mathbf{k}) &= w_\mathbf{q}^b(\mathbf{k}) \\ &\quad + \frac{1}{\epsilon(q)} \left[v_{dq+} + \frac{2}{\pi^2 q^2} \int_{k\leqslant k_F} d^3k \, \frac{|N_\mathbf{k}|^2 w_\mathbf{q}^b(\mathbf{k})}{E_\mathbf{k}^{(0)} - E_{\mathbf{k}+\mathbf{q}}^{(0)}} \right], \end{aligned} \tag{15}$$

where

$$\epsilon(q) = 1 - \frac{2}{\pi^2 q^2} \int_{k\leqslant k_F} d^3k \, \frac{|N_\mathbf{k}|^2}{E_\mathbf{k}^{(0)} - E_{\mathbf{k}+\mathbf{q}}^{(0)}}, \tag{16}$$

which, in the local pseudopotential theory, reduces to the well-known Lindhard dielectric function. Note that the above derivation for the screened electron density is within the random phase approximation. The inclusion of EC corrections runs almost in parallel. For example, one writes the valence electron density with EC effects included (denoted by a superscript EC) as

$$\begin{aligned} \langle \mathbf{k}+\mathbf{q}|n^{\mathrm{EC}}(\mathbf{r})|\mathbf{k}\rangle &= \wp(q) \left[\frac{1}{2\pi^3} \int_{k\leqslant k_F} d^3k \, \frac{|N_\mathbf{k}|^2 w_\mathbf{q}^{\mathrm{EC}}(\mathbf{k})}{E_\mathbf{k}^{(0)} - E_{\mathbf{k}+\mathbf{q}}^{(0)}} \right] \\ &\quad + \wp(q) \rho_q \end{aligned} \tag{17}$$

and using the relation as suggested by Shaw [24], we introduce the local field EC factor $F(q)$ into Eq. (7) as

$$\begin{aligned} \langle \mathbf{k}+\mathbf{q}|V_e^{\mathrm{EC}}(\mathbf{r})|\mathbf{k}\rangle &\equiv \wp(q) v_e^{\mathrm{EC}}(q) \\ &= \frac{4\pi}{q^2} \langle \mathbf{k}+\mathbf{q}|n^{\mathrm{EC}}(\mathbf{r})|\mathbf{k}\rangle [1 - F(q)]. \end{aligned} \tag{18}$$

The screened form factor with the EC corrections then reads

$$w_\mathbf{q}^{\mathrm{EC}}(\mathbf{k}) = w_\mathbf{q}(\mathbf{k}) - \frac{F(q)}{\tilde{\epsilon}(q)} v_e(q) \tag{19}$$

in which $\tilde{\epsilon}(q) = 1 + [\epsilon(q) - 1][1 - F(q)]$. After simplification, we arrive at

$$n^{\mathrm{EC}}(q) = \frac{1}{\tilde{\epsilon}(q)} \left[\frac{1}{2\pi^3} \int_{k\leqslant k_F} d^3k \, \frac{|N_\mathbf{k}|^2 w_q^b(\mathbf{k})}{E_\mathbf{k}^{(0)} - E_{\mathbf{k}+\mathbf{q}}^{(0)}} + \frac{q^2}{4\pi} v_{dq} \right], \tag{20}$$

which is the screened electron charge density defined by $\langle \mathbf{k}+\mathbf{q}|n^{\mathrm{EC}}(\mathbf{r})|\mathbf{k}\rangle = \wp(q) n^{\mathrm{EC}}(q)$ and used in the following calculation. It is interesting to note that when the pseudopotential is taken to be local, v_{dq} vanishes, $w_\mathbf{q}^b(\mathbf{k})$ becomes k independent [such as the bare-ion form factor of the Ashcroft empty core potential [25], $w_\mathbf{q}^b = -4\pi Z \cos(r_c q)/(\Omega_0 q^2)$, r_c being an adjustable parameter representing an effective core radius], and the result leads exactly to the expression in the local pseudopotential approximation [13].

C. Ion-ion static structure factor

We are now left with the determination of the ion-ion static structure factor. This quantity, which describes ion-ion correlations in the presence of other ions and also of the interacting valence electron gas can be calculated in many different methods. Here we have chosen the modified hypernetted-chain (MHNC) integral equation approach, since this approach has been previously examined by us to be quite reliable. In this section we only summarize those essential equations that are needed in the following discussion; for complete documentation the reader is referred to original works for details [18,26].

1. Interatomic potential

An important ingredient in the MHNC theory is the interionic potential $\phi(r)$. As pointed out above, we shall use the generalized EINMP theory [16] to construct $\phi(r)$. According to Wang and Lai [17], $\phi(r)$ can be written as

$$\phi(r) = \frac{Z_{\mathrm{eff}}^2}{r} \left[1 - \frac{2}{\pi} \int_0^\infty dq G_N(q) \, \frac{\sin qr}{q} \right], \tag{21}$$

where $G_N(q)$ is the normalized energy-wave-number characteristics in which is included the EC factor and $Z_{\mathrm{eff}}^2 = Z^2 - \rho_d^2$. It is worthwhile to emphasize that in applying Eq. (21) we have followed Li *et al.* [16] by incorporating through the one-electron energy and pseudo wave function (via a model potential parameter β) the higher (than second) order corrections into the bare-ion pseudopotential. The rigorousness and reliability of such a procedure have been critically assessed in a series of successful applications to various metallic properties [18,26]. For all liquid metals considered here we have attempted three EC corrections, namely, those of Singwi *et al.* [27], Ichimaru and Utsumi [28], and Moroni *et al.* [2]. These three local field factors are representative of theories developed in the period 1970–1990.

2. Modified hypernetted-chain theory

Having introduced $\phi(r)$, we turn to discuss the pair correlation function $g(r)$ in the integral equation approach. The study of $g(r)$ at given temperature T and number density ϱ_i can be obtained from the Ornstein-Zernike relation defined by

$$\gamma(r) \equiv h(r) - c(r) = \varrho_i \int h(\mathbf{r}') c(|\mathbf{r}-\mathbf{r}'|) d\mathbf{r}' \qquad (22)$$

in which $h(r) = g(r) - 1$ and $c(r)$ is the total and direct correlation functions, respectively. To solve Eq. (22) one must supplement it with a closure between $h(r)$ and $c(r)$. A formally exact closure relation is

$$g(r) = \exp[\gamma(r) - \phi(r)/(k_B T) - B(r)], \qquad (23)$$

where the bridge function $B(r)$ (equal to zero for the usual hypernetted-chain approximation) is the sum of the "bridge" diagrams [29]. Given $\phi(r)$ the pair correlation function can be determined by iteratively solving Eqs. (22) and (23) for a prescription of the function $B(r)$. In this work we have employed a highly accurate hard-sphere $B(r)$ proposed previously by Malijevský and co-workers [30]. In their original works these authors assumed an empirical analytic expression for $B(r)$, which is given as $B(r) = b^2(r)$, where

$$b(r) = \begin{cases} [a_1 + a_2(r/\sigma - 1)][r/\sigma - 1 - a_3][r/\sigma - 1 - a_4]/(a_3 a_4), & r \leqslant a_4\sigma \\ A_1 \exp[-a_5(r/\sigma - 1 - a_4)] \sin[A_2(r/\sigma - 1 - a_4)]/r, & r \geqslant a_4\sigma \end{cases} \qquad (24)$$

where σ is the hard-sphere diameter, and A_i and a_i are constants determined, respectively, by continuity conditions and by fitting to computer simulation data of all known structural and thermodynamic properties of hard spheres over the entire fluid range up to the density of freezing. Thus, $B(r)$ given by Eq. (24) ensures agreement with simulation data of hard spheres and is therefore an accurate empirical hard-sphere bridge function that has in fact been shown by us in one recent work [26].

III. NUMERICAL RESULTS AND DISCUSSION

We turn now to a discussion of our numerical results. As shown in Eq. (5) the electron-ion structure factor to the first order in electron-ion interaction is the product of the screened electron charge density and ion-ion static structure factor. It would therefore be more instructive if we first examine the change in each quantity and see how it contributes to $S_{ei}(q)$.

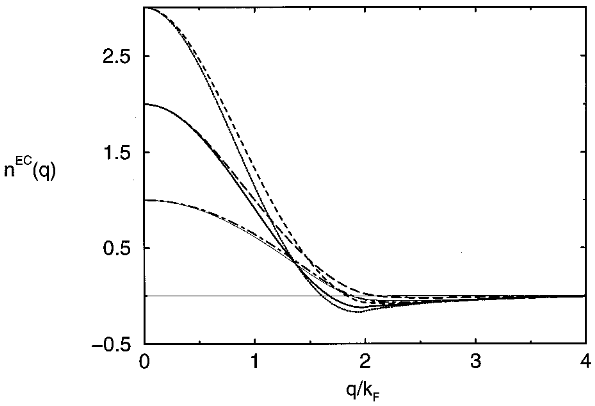

FIG. 1. Screened electron charge density $n^{EC}(q)$ for liquid metals Na (thin full curve), Rb (dot-dashed curve), Mg (thick full curve), Zn (long-dashed curve), Al (dotted curve), and Ga (short-dashed curve) calculated using the generalized EINMP and exchange-correlation factor of Ichimaru and Utsumi [28].

A. Numerical results of $n^{EC}(q)$

Figure 1 reports our $n^{EC}(q)$ for the six liquid metals, namely, Na, Rb, Mg, Zn, Al, and Ga, calculated using the generalized EINMP theory [16] and for convenience in comparison with experiments, with the EC factor of Ichimaru and Utsumi [28] [which is the only local field factor used experimentally to extract $S_{ei}(q)$ [1]] included in the model pseudopotential. These materials are representative of monovalent, divalent, and trivalent metals and, respectively, they are in the order of increasing electronic density. Two distinct features are observed.

(a) For the nearly-free-electron-like liquid metals to which Al, Mg, Na, and Rb belong, the $n^{EC}(q)$ of trivalent, divalent, and monovalent metals each decreases from their respective valence and crosses zero quite generally in the order of Al→Mg→(Na, Rb) with Al and Mg showing clear first minima, but those of Na and Rb are weakly visible. In contrast, nonsimple liquid metals such as Zn, which exhibits an asymmetry in the principal peak of $S_{ii}(q)$ [18] and Ga, which contains a shoulderlike structure on the falling edge of $S_{ii}(q)$ [31], separately displays a totally different behavior. Although the trend in crossing zero is similar, first trivalent metal Ga and then divalent metal Zn, the points of crossing zeros are located at a larger q.

(b) For the four polyvalent liquid metals, the $n^{EC}(q)$ of nearly-free-electron metals (Al, Mg) decay more rapidly than the nonsimple liquid metals (Ga, Zn), which each shows an initial stretched $n^{EC}(q)$ accompanied by a weakly oscillatory damped tail.

As will be seen below, feature (a) is crucial for understanding the structure of $S_{ei}(q)$. The node of $n^{EC}(q)$ for each liquid metal is intimately related to the node of its pseudopotential if the latter is assumed to be local. This can be seen quite easily if one goes back to Eq. (20) and note that in the local pseudopotential approximation v_{dq} is identically zero and $n^{EC}(q)$ is directly proportional to $w^b_{\mathbf{q}}$. On the other hand, for a nonlocal pseudopotential, $v_{dq} \neq 0$ (since $M(q) \neq 0$ for a nonlocal pseudopotential) the location of the node will thus

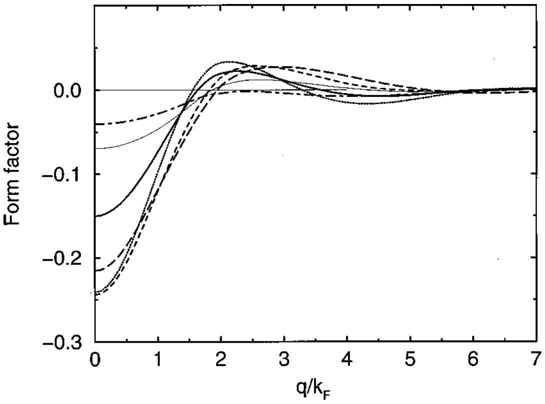

FIG. 2. Pseudopotential form factor for six liquid metals Na (thin full curve), Rb (dot-dashed curve), Mg (thick full curve), Zn (long-dashed curve), Al (dotted curve), and Ga (short-dashed curve).

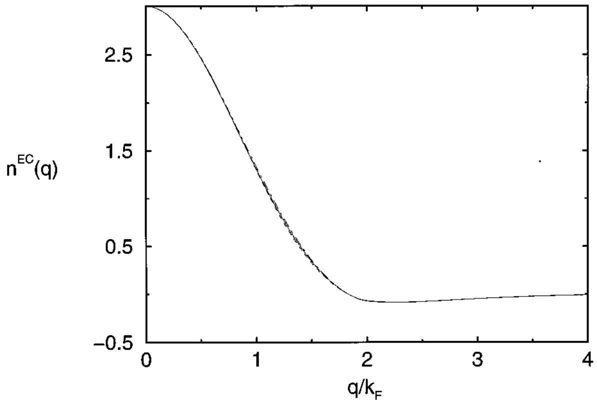

FIG. 4. Screened electron charge density $n^{\mathrm{EC}}(q)$ for liquid metal Ga calculated with the EC factors of Singwi *et al.* [27] (dashed curve) and Moroni *et al.* [2] (full curve) compared with that of Ichimaru and Utsumi [28] (dot-dashed curve).

have a delicate effect on $n^{\mathrm{EC}}(q)$. We show in Fig. 2 the variation of our pseudopotential form factor for the six liquid metals of interest here. The correlation between the nodes in $n^{\mathrm{EC}}(q)$ and $w_{\mathbf{q}}^{\mathrm{EC}}(\mathbf{k})$ are less regular. In regard to feature (b) the general structures displayed in Fig. 1 physically suggest that the distributions of valence electrons in Al and Mg are somewhat diffused compared with those of Ga and Zn whose spatial distributions are relatively more compact. It is perhaps noteworthy to remark that, although the use of different EC factors to account quantitatively for the electron-electron interactions do have significant effects on metallic properties such as the phonon spectra, electrical resistivity, interionic interactions [and hence the $S_{ii}(q)$ [18]] etc., its role on $n^{\mathrm{EC}}(q)$ appears to be inconsequential. To see this, we depict in Fig. 3 the pair potentials for Ga calculated using the local field factors of Singwi *et al.* [27], Moroni *et al.* [2], and Ichimaru and Utsumi [28]. Similar comparison for the EC corrections in liquid metal Zn at $T=723$ K was given previously in Fig. 4 of [18]. These figures clearly manifest the sensitivity of $\phi(r)$ on the local field factor. In contrast, there seems to be virtually no change in $n^{\mathrm{EC}}(q)$ with different EC corrections (see Fig. 4). Nevertheless one should notice further that, among different liquid metals, the results in feature (b) are in fact indicative of the combined effects of electron-electron interactions, which are shown above to be insensitive to $n^{\mathrm{EC}}(q)$ and of nonlocality of electronic pseudopotential, which we believe is an important piece of information for understanding the electron-ion correlation. We shall discuss this more in the next section.

B. Numerical results of $S_{ii}(q)$

To facilitate a direct comparison among the six liquid metals, we plot in Fig. 5 the $S_{ii}(q)$ versus q all scaled to their respective Fermi wave vector. It is interesting to notice immediately that in going along the trend, monovalent→divalent→trivalent, the first peak position q_m of $S_{ii}(q)$, with respect to $q=2k_F$, shifts systematically inward—the monvalent metals (Na, Rb) have their $q=2k_F$ lying half-way at the rising edge before q_m, the divalent metals (Mg, Zn) lying just after q_m, while those of trivalent metals (Al, Ga) lying beyond q_m. That $q=2k_F$ is judiciously chosen for comparison is because in the vicinity of this point different local field factors deviate most and $n^{\mathrm{EC}}(q)$ drops nearly to zero.

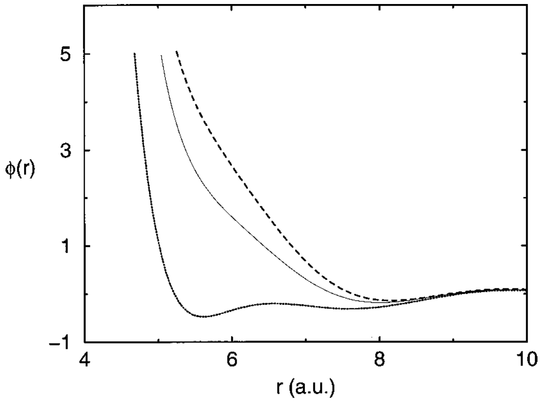

FIG. 3. Interionic pair potential $\phi(r)$ (in units of k_BT) for liquid metals Ga calculated with the EC factor of Singwi *et al.* [27] (dotted curve), Moroni *et al.* [2] (full curve) compared with that of Ichimaru and Utsumi [28] (dashed curve).

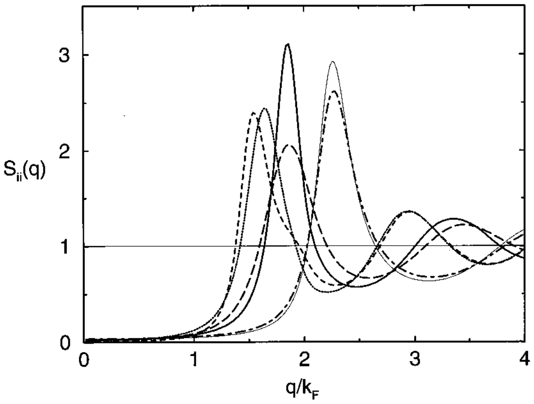

FIG. 5. Static structure factor $S(q)$ for liquid metals Na (thin full curve), Rb (dot-dashed curve), Mg (thick full curve), Zn (long-dashed curve), Al (dotted curve), and Ga (short-dashed curve) calculated using the MHNC with $B(r)$ of Malijevský *et al.* [30] and $\phi(r)$, which includes the EC factor of Ichimaru and Utsumi [28].

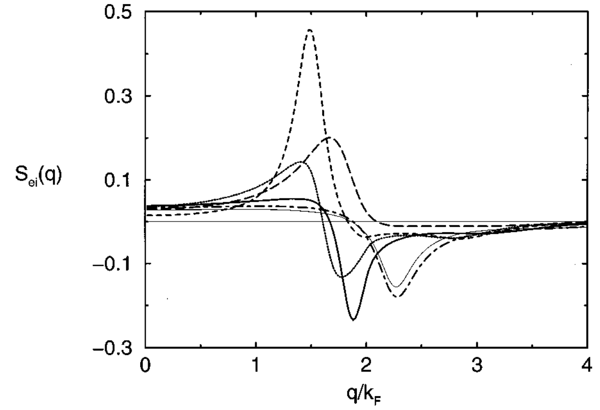

FIG. 6. Electron-ion structure factor $S_{ei}(q)$ for liquid metals Na (thin full curve), Rb (dot-dashed curve), Mg (thick full curve), Zn (long-dashed curve), Al (dotted curve), and Ga (short-dashed curve) calculated using Eq. (5) for the EC factor of Ichimaru and Utsumi [28].

C. Numerical results of $S_{ei}(q)$

We are now in a position to discuss the structure of $S_{ei}(q)$ for the six liquid metals that are all delineated in Fig. 6. There are two general points that merit emphasis.

(a) For all of the liquid metals, $S_{ei}(q)$ changes quite generally, first increasing at small q, going through a maximum, and then descenting through the zero to a minimum, and finally continuing by a weakly damped oscillation.

(b) There is no systematic trend for tracing the positions of first maximum and first minimum of $S_{ei}(q)$ purely from a knowledge of the electron density in liquid metals.

It is not difficult to understand point (a) if one recalls the positions of the main maxima of $S_{ii}(q)$ and the way $n^{\mathrm{EC}}(q)$ goes to zero. For the divalent and trivalent liquid metals, because of the behavior in $S_{ii}(q)$ noted in Sec. III B, the first maximum of $S_{ei}(q)$ comes mainly from the contribution of the principal peak of $S_{ii}(q)$, which is either enhanced or diminished by $n^{\mathrm{EC}}(q)$ depending on how slow or how fast it decays. Quite generally, the positions of the first peaks of $S_{ei}(q)$ for these elements lie slightly to the left of q_m. On the other hand, for the monovalent liquid alkali metals, the locations of their $n^{\mathrm{EC}}(q)$'s minima are near q_m, which thus leads to clear first minima of $S_{ei}(q)$. An important aspect to emphasize is the node of $S_{ei}(q)$, which is exactly the same as that of $n^{\mathrm{EC}}(q)$ since $S_{ii}(q)$ is positive definite. From Eq. (20), one would therefore expect in general a full nonlocal pseudopotential theory to predict a $S_{ei}(q)$ different from that in the local pseudopotential theory. This is illustrated in Fig. 7 for the $n^{\mathrm{EC}}(q)$ of three of the liquid metals considered here [32]. Lastly, for the damped oscillatory behavior it can be attributed to the matching of $S_{ii}(q)$ and $n^{\mathrm{EC}}(q)$ and its magnitude depends on whether they are in phase or out of phase. It is interesting to note that the first minimum of $n^{\mathrm{EC}}(q)$ corresponds closely to the principal minimum of $S_{ei}(q)$, a feature that is found to be generally true ($\lesssim 10\%$) for all of the six liquid metals. Coming to point (b), this simply reflects the delicate manner in computing $S_{ei}(q)$; a slight change in curvature of $n^{\mathrm{EC}}(q)$ can lead to subtle different structure of $S_{ei}(q)$ [see Fig. 7 for a comparison of the $n^{\mathrm{EC}}(q)$ of local [32] and nonlocal pseudopotential theories].

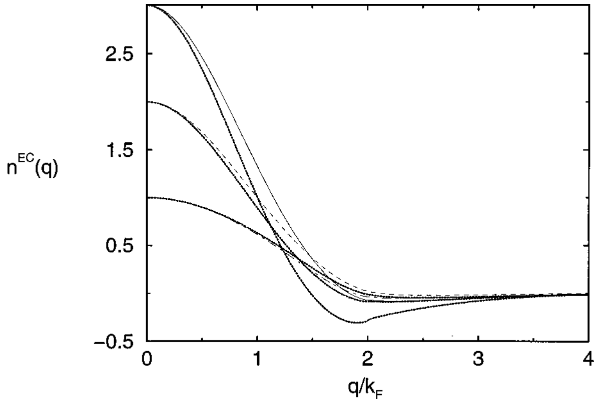

FIG. 7. Screened electron charge density $n^{\mathrm{EC}}(q)$ for liquid metals Ga (full curve), Zn (dashed curve), and Na (dot-dashed curve) calculated with the generalized EINMP theory with the EC factor of Ichimaru and Utsumi [28] compared with those calculated with the empty core local pseudopotential given by dotted curves. The Ashcroft empty core radii are taken from [35] for Zn and Na, and from [36] for Ga.

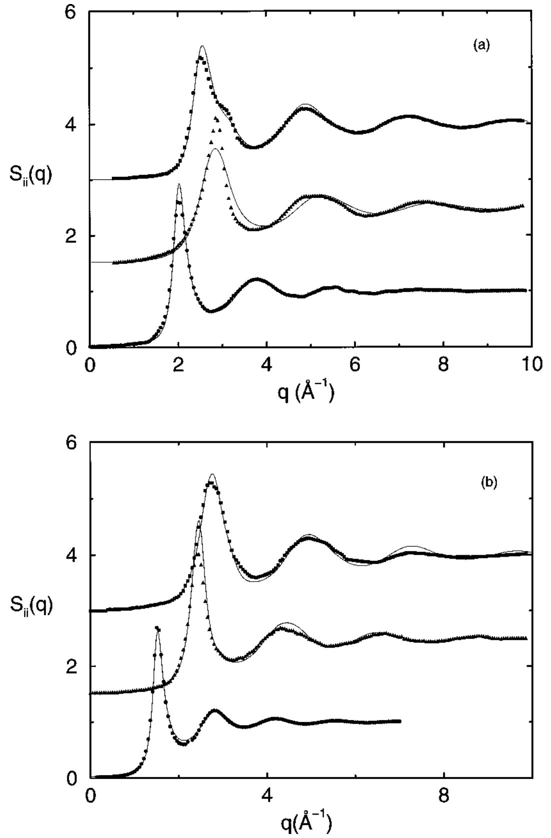

FIG. 8. (a) Static structure factor $S_{ii}(q)$ for liquid metals Na, Zn, and Ga calculated using the MHNC (see text) compared with the experimental results of Takeda [1]. The theoretical results are given by full curves and experimental neutron scattering data are Na (circles), Zn (triangles), and Ga (squares). (b) Static structure factor $S_{ii}(q)$ for liquid metals Rb, Mg, and Al calculated using the MHNC (see text) compared with the experimental results of Takeda [1] and Waseda [34]. The theoretical results are given by full curves and experimental neutron scattering data are Mg (triangles) and Al (squares). Note that the x-ray data for Rb (circles) are taken from [34] measured at 313 K.

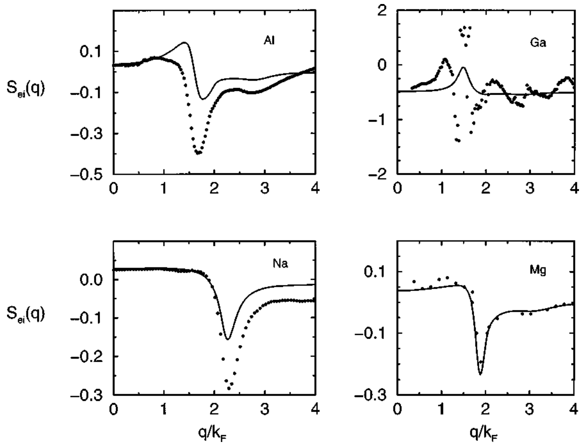

FIG. 9. Electron-ion structure factor $S_{ei}(q)$ for liquid metals Al, Ga, Mg, and Na calculated using Eq. (5) with the EC factor of Ichimaru and Utsumi [28]. The theoretical results are given by full curves compared with those of experiments [1] or simulation data [5] by solid circles.

At this point, it is perhaps appropriate to ask the following: (1) How do our calculated results compare with experiments? (2) How important is the nonlocality of valence electrons on $n^{\mathrm{EC}}(q)$ having checked above that the EC factor is insignificant? For question (1), there are two sets of data to be compared. In Fig. 8, we display our calculated $S_{ii}(q)$ compared with those of neutron scattering [1] or x-ray diffraction experiments [33] and in Fig. 9 we show our results of $S_{ei}(q)$ along with the experimental data extracted by Takeda and co-workers [1]. For the $S_{ii}(q)$, the overall agreement is excellent for liquid alkali metals, and the compatibility is favorably good also for liquid polyvalent metals, apart from the magnitudes of first peaks and a shift in the first minimum position for Zn. The discrepancies for the $S_{ii}(q)$ of liquid polyvalent metals, in particular Zn, are hard to assess since experimental errors for these elements are generally larger and more susceptible to uncertainties. We therefore feel that the structures of $S_{ii}(q)$ predicted in our work are reasonably in order. As regards the $S_{ei}(q)$, our theoretical findings interpret very well the various positions of extrema of $S_{ei}(q)$. It thus appears that the generalized EINMP used self-consistently in this work for the calculation of $n^{\mathrm{EC}}(q)$ and $S_{ii}(q)$ is basically correct. Specifically it is encouraging to mention our results for Ga and Mg. For the former, its $S_{ei}(q)$ shows the same anomalous sharp positive maximum as Boulahbak *et al.* [14] who applied the Shaw's nonlocal optimized model potential theory [24] and for the latter it compares very well with the first-principles molecular dynamics simulation of de Wijs *et al.* [5].

Turning now to question (2), this feature may be worth examining since we are looking at the correlation between electrons and ions. We have in fact addressed this problem in Sec. II B by drawing attention to the state dependence of valence electrons and accounting for the oscillatory part of the true wave functions localized in the ion core region Ω_c by the depletion charge density. With further consideration of a tractable means in obtaining the depletion charge density function, we are led to introduce the modulation function $M(q)$, which essentially dictates the depletion hole charge distribution within Ω_c. Unfortunately there are not many works in the literature that study the detailed nature of this quantity. The main difficulty lies in the fundamental aspect of this function, which requires a knowledge of the real wave functions within Ω_c. But the latter are just precisely the target that the model pseudopotential theory is trying to avoid. Accordingly we may have to examine $M(q)$ by a qualitative but nonetheless reasonable means. Three related calculations are relevant; these are the studies of bulk moduli of simple metals by Pynn [21], of electronic and dynamic properties of the simple metal aluminum by Rao [22], and of thermodynamic properties of liquid metals by Kumaravadivel [23]. Now the conclusions reached by these authors may serve as a useful guide for us to evaluate the importance of $M(q)$. First, the form for $M(q)$ is nonunique but must be chosen such that the total depletion charge should be located within Ω_c in which the pseudo and true wave functions differ. Several forms of $M(q)$ that satisfy this property are (a) zero depletion hole charge, $M(q)=0$, which corresponds to the local pseudopotential theory, (b) delta function distribution, $M(q)=1$, (c) Shaw's form [24], $M(q)=1/[1+(q/k_F)^2]$, where k_F is the Fermi wave vector, (d) Pynn's form [21], $M(q)=\exp[-(q\mathcal{R}_c)^2/4\zeta]$ in which $1\leqslant\zeta\leqslant 4$, and (d) uniform depletion charge distribution, $M(q)=3[\sin q\mathcal{R}_c/(q\mathcal{R}_c)-\cos q\mathcal{R}c]/(q\mathcal{R}_c)^2$ [37], which is the one widely used and employed in all the above calculations. Second, the inclusion of the nonpoint depletion charge has a considerable effect on the energy wave-number characteristic and hence the interatomic potential. This property of $M(q)$ was shown explicitly in the works of Pynn for the $G^{\mathrm{EC}}(q)$ (see Fig. 1 of [21]) and binding energy (for Al about 20% difference), and of Kumaravadivel [23] for the excess entropy, long wavelength limit of the structure factor, and $\phi(r)$ (see Fig. 4 and Table 14 of [23]). Third, the effect of using different nonpoint $M(q)$'s is still found to be discernible, although less significant. The specific physical properties that have been examined include the electronic [22] and thermodynamic [21,23] quantities such as the interionic potential, electrical resistivity (less than 5%), excess entropy (less than 10%), constant volume specific heat, and bulk modulus (both less than 5%). Fourth, when different forms of $M(q)$ are compared the calculated physical quantity straddles the experimental values (see [22,23] for specific examples).

Within the context of the nonlocal pseudopotential theory, it is implied from these remarks that the effect of any nonpoint $M(q)$ is inconsequential in the general structure of $S_{ei}(q)$; one would not expect too big a difference in the electron-ion correlation if different forms of $M(q)$ are attempted. We have in fact checked on this aspect by repeating the above calculation for $n^{\mathrm{EC}}(q)$ using Pynn's form of $M(q)$. By choosing $\zeta=2$, which is a value that best agrees with measurements generally, we virtually find no difference in the $n^{\mathrm{EC}}(q)$ for liquid metals Mg and Zn compared with the uniform depletion charge distribution. On physical grounds, the choice of different $M(q)$'s on $S_{ei}(q)$ for liquid alkali metals is going to be even smaller. Thus, one is comfortably safe for the $S_{ei}(q)$ results against $M(q)$ if one is applying a nonlocal pseudopotential theory. This conclusion further explains why our results for the alkalis and Ga are the of the same quality as those of Boulahbak *et al.* [14].

IV. CONCLUSION

Following the functional derivative method of Cusack *et al.* [19] we first obtain an equation for the electron-ion correlation expressed in terms of a product of the screened electron charge density and ion-ion static structure factor. A full nonlocal model pseudopotential with three different EC factors is then employed to construct the former and the integral equation approach based on the modified hypernetted-chain approximation is applied self-consistently to determine the latter. The $S_{ei}(q)$ for six liquid metals near their respective freezing temperatures are calculated and they are seen to interpret favorably the measured data of Takeda [1]. In analyzing various contributions to $S_{ei}(q)$, we find that the calculated $S_{ii}(q)$ for the liquid alkalis compare very well with experiments whereas for those of the polyvalent liquid metals the agreement with observed data is in good reasonable order. While for the $n^{\mathrm{EC}}(q)$, we point out that the electron-ion structure factor calculated using the local pseudopotential theory is formally different from that within the context of nonlocal pseudopotential theory. One main difference lies in the depletion hole charge distribution, which has a non-negligible effect on $n^{\mathrm{EC}}(q)$ and $S_{ii}(q)$, and hence on $S_{ei}(q)$. Given a nonlocal pseudopotential our calculation indicates that different EC factors or $M(q)$'s have a less significant influence on $n^{\mathrm{EC}}(q)$ and $S_{ii}(q)$ and the corresponding $S_{ei}(q)$'s are thus quite similar.

ACKNOWLEDGMENTS

We gratefully acknowledge the financial support from the Hiroshima City University grant under which the present project was initiated, and from the National Science Council of Taiwan, ROC (Grant No. NSC87-2112-M-008-004) under which the project has continued. S.K.L. would like to thank Hiroshima City University, Professor M. Iwamatsu, in particular, for his kind hospitality, and the Australian Academy of Science with the National Science Council of Taiwan, ROC, for an opportunity to participate in an Academies' exchange program under which part of this work was written. We also thank the National Center for High-Performance Computing of Taiwan, ROC, for their continual support of computing resources.

---

[1] S. Takeda *et al.*, J. Phys. Soc. Jpn. **55**, 3437 (1986); **55**, 184 (1986); **58**, 3999 (1989); **60**, 2241 (1991); **63**, 1794 (1994).

[2] S. Moroni, D. Ceperley, and G. Senatore, Phys. Rev. Lett. **69**, 1837 (1992).

[3] G. Ortiz and P. Ballone, Phys. Rev. B **50**, 1391 (1994).

[4] C. F. Richardson and N. W. Ashcroft, Phys. Rev. B **50**, 8170 (1994).

[5] G. A. de Wijs, G. Pastore, A. Selloni, and W. van der Lugt, Phys. Rev. Lett. **75**, 4480 (1995).

[6] F. Shimojo, Y. Zempo, K. Hoshino, and M. Watabe, Phys. Rev. B **52**, 9320 (1995), and references cited therein.

[7] R. D. Cowan and J. G. Kirkwood, J. Chem. Phys. **29**, 264 (1958).

[8] M. P. Tosi and N. H. March, Nuovo Cimento B **15**, 308 (1973); F. Vericat, G. Pastore, and M. P. Tosi, Nuovo Cimento D **8**, 59 (1986).

[9] M. Watabe and M. Hasegawa, *Second International Conference on Liquid Metals* (Taylor and Francis, New York, 1973), p. 133.

[10] J. Chihara, *Second International Conference on Liquid Metals* (Taylor and Francis, New York, 1973), p. 137.

[11] S. A. Trigger, Phys. Lett. **56A**, 325 (1976).

[12] J. Chihara, J. Phys. F **17**, 295 (1987); M. Ishitobi and J. Chihara, J. Phys.: Condens. Matter **4**, 3679 (1992).

[13] K. Hoshino and M. Watabe, J. Phys. Soc. Jpn. **61**, 1663 (1992). Note that the dielectric function given in this work should be more correctly referred to the proton dielectric function [V. Heine and I. Abarenkov, Philos. Mag. **9**, 451 (1964)].

[14] J. F. Wax, N. Jakse, and J. L. Bretonnet, Phys. Rev. B **55**, 12 099 (1997); M. Boulahbak, J. F. Wax, N. Jakse, and J. L. Bretonnet, J. Phys.: Condens. Matter **9**, 4017 (1997).

[15] To ensure the validity of the linear response approximation, we have here given a proper attention to the higher than second order corrections in our perturbation theory. Within the context of the generalized energy independent nonlocal model pseudopotential theory (Ref. [16] below), this can be achieved by a unitary transformation of the pseudowave function, which, through the matrix element of the electron-ion pseudopotential, will fold back the third and higher order contributions to the one-electron energy via a model potential parameter β. Thus although the *forms* of the one-electron energy and wave function are the same as in the usual perturbation theory, the physical content of them is not the same. This procedure of incorporating many-body effects has been compared with standard direct third order perturbation calculations [C. M. Bertoni, V. Bortolani, G. Caglioti, K. R. Rao and A. D. B. Woods, Phys. Rev. **128**, 1099 (1962); L. Dagens, M. Rasolt, and R. Taylor, Phys. Rev. B **11**, 2726 (1975)] for the phonon spectra of sp metals. The good agreement of the calculated results with measured values lends great credence to the present perturbation theory. One should be cautious in the use of the linear response approximation when effects of *s-d* hybridization (such as the alkali earth metals or transition metals) or *sp* mixing (such as the lithium metal) are important. The readers may consult the works of D. H. Li, R. A. Moore, and S. Wang (Can. J. Phys. **64**, 75 (1986); **64**, 852 (1986)) for technical details.

[16] D. H. Li, X. R. Li, and S. Wang, J. Phys. F **16**, 309 (1986); D. H. Li, R. A. Moore, and S. Wang, J. Phys. F **17**, 2007 (1987).

[17] S. Wang and S. K. Lai, J. Phys. F **10**, 2717 (1980).

[18] S. K. Lai, Wang Li, and M. P. Tosi, Phys. Rev. A **42**, 7289 (1990). Reference [47] in this paper gives a detailed listing of the previous applications.

[19] S. Cusack, N. H. March, M. Parrinello, and M. P. Tosi, J. Phys. F **6**, 749 (1976).

[20] R. W. Shaw and W. A. Harrison, Phys. Rev. **163**, 604 (1967).

[21] R. Pynn, Phys. Rev. B **5**, 4826 (1972).

[22] P. V. S. Rao, J. Phys. Chem. Solids **35**, 669 (1974).

[23] R. Kumaravadivel, J. Phys. F **13**, 1607 (1983).

[24] R. W. Shaw, Phys. Rev. **174**, 769 (1968); J. Phys. C **3**, 1140 (1970).

[25] N. W. Ashcroft, J. Phys. C **1**, 232 (1968).

[26] H. C. Chen and S. K. Lai, Phys. Rev. E **49**, R982 (1994); Phys. Rev. A **45**, 3831 (1992).

[27] K. S. Singwi, A. Sjölander, M. P. Tosi, and R. H. Land, Phys. Rev. B **1**, 1044 (1970).

[28] S. Ichimaru and K. Utsumi, Phys. Rev. B **24**, 7385 (1981).

[29] J. P. Hansen and I. R. MacDonald, *The Theory of Simple Liquids* (Academic, London, 1986).

[30] A. Malijevský, S. Labík, and W. R. Smith, Mol. Phys. **72**, 193 (1991); **60**, 663 (1987); **67**, 431 (1989).

[31] H. C. Chen and S. K. Lai, Phys. Rev. E **56**, 4381 (1997).

[32] We have not attempted to compare the $S_{ei}(q)$ since the $S_{ii}(q)$ has to be self-consistently determined with the same local pseudopotential. It should not be difficult, however, to see the sensitivity of matching between $n^{\mathrm{EC}}(q)$ and $S_{ii}(q)$ that leads to $S_{ei}(q)$.

[33] When compared with the x-ray data, we are in fact assuming a negligible difference in the form factors of neutral atoms and pseudoatoms. Recent work by J. Chihara and S. Kambayashi [J. Phys.: Condens. Matter **6**, 10221 (1994)] gives numerical evidences for the cases of liquid alkali metal and Al.

[34] Y. Waseda, *The Structure of Non-Crystalline Materials* (McGraw-Hill, New York, 1980).

[35] C. Regnaut, J. Phys. F **16**, 295 (1986).

[36] M. C. Bellissent-Funel, R. Bellissent, and G. Tourand, J. Phys. F **11**, 139 (1981).

[37] M. Appapillai and V. Heine, Cavendish Laboratory, Cambridge Technical Report No. 5 (1972).